

RESEARCH ARTICLE

Development of a Mild Viral Expression System for Gain-Of-Function Study of Phytoplasma Effector *In Planta*

Sin-Fen Hu¹, Yu-Hsin Huang⁴, Chan-Pin Lin⁴, Li-Yu Daisy Liu⁶, Syuan-Fei Hong⁵, Chiao-Yin Yang⁴, Hsiao-Feng Lo⁵, Ting-Yu Tseng⁷, Wei-Yao Chen¹, Shih-Shun Lin^{1,2,3*}

1 Institute of Biotechnology, National Taiwan University, Taipei, Taiwan, **2** Genome and Systems Biology Degree Program, National Taiwan University, Taipei, Taiwan, **3** Agricultural Biotechnology Research Center, Academia Sinica, Taipei, Taiwan, **4** Department of Plant Pathology and Microbiology, National Taiwan University, Taipei, Taiwan, **5** Department of Horticulture and Landscape Architecture, National Taiwan University, Taipei, Taiwan, **6** Department of Agronomy, National Taiwan University, Taipei, Taiwan, **7** Joint Center for Instruments and Researches, College of Bioresources and Agriculture, National Taiwan University, Taipei, Taiwan

☞ These authors contributed equally to this work.

* linss01@ntu.edu.tw



OPEN ACCESS

Citation: Hu S-F, Huang Y-H, Lin C-P, Liu L-YD, Hong S-F, Yang C-Y, et al. (2015) Development of a Mild Viral Expression System for Gain-Of-Function Study of Phytoplasma Effector *In Planta*. PLoS ONE 10(6): e0130139. doi:10.1371/journal.pone.0130139

Academic Editor: Keith R. Davis, Indiana University, UNITED STATES

Received: December 29, 2014

Accepted: May 18, 2015

Published: June 15, 2015

Copyright: © 2015 Hu et al. This is an open access article distributed under the terms of the [Creative Commons Attribution License](https://creativecommons.org/licenses/by/4.0/), which permits unrestricted use, distribution, and reproduction in any medium, provided the original author and source are credited.

Data Availability Statement: All relevant data are within the paper and its Supporting Information files. The raw transcriptome reads of Col-0 and SAP54 plants are available in the NCBI Short Read Archive under accession number SRR1979100 (normal flower of Col-0 plant), and SRR1979105 (leafy flower of SAP54 plant).

Funding: This study was supported by grants NSC-102-2313-B-002-068-MY3, NSC-102-2313-B-002-066-B-MY3, and NSC-103-2313-B-002-007 from the Ministry of Science and Technology, Taiwan; and 104R7602B2 from National Taiwan University.

Abstract

PHYL1 and SAP54 are orthologs of pathogenic effectors of Aster yellow witches'-broom (AYWB) phytoplasma and Peanut witches'-broom (PnWB) phytoplasma, respectively. These effectors cause virescence and phyllody symptoms (hereafter leafy flower) in phytoplasma-infected plants. T₀ lines of transgenic Arabidopsis expressing the *PHYL1* or *SAP54* genes (*PHYL1* or *SAP54* plants) show a leafy flower phenotype and result in seedless, suggesting that PHYL1 and SAP54 interfere with reproduction stage that restrict gain-of-function studies in the next generation of transgenic plants. *Turnip mosaic virus* (TuMV) mild strain (TuGK) has an Arg182Lys mutation in the helper-component proteinase (HC-Pro^{R182K}) that blocks suppression of the miRNA pathway and prevents symptom development in TuGK-infected plants. We exploited TuGK as a viral vector for gain-of-function studies of *PHYL1* and *SAP54* in Arabidopsis plants. TuGK-PHYL1- and TuGK-SAP54-infected Arabidopsis plants produced identical leafy flower phenotypes and similar gene expression profiles as *PHYL1* and *SAP54* plants. In addition, the leafy flower formation rate was enhanced in TuGK-PHYL1- or TuGK-SAP54-infected Arabidopsis plants that compared with the T₀ lines of *PHYL1* plants. These results provide more evidence and novel directions for further studying the mechanism of PHYL1/SAP54-mediated leafy flower development. In addition, the TuGK vector is a good alternative in transgenic plant approaches for rapid gene expression in gain-of-function studies.

Competing Interests: The authors have declared that no competing interests exist.

Introduction

Aster yellow witches'-broom (AYWB) phytoplasma causes virescence and phyllody symptoms in host plants [1]. Maclean et al. (2011) individually expressed several putative secreted AYWB phytoplasma proteins (SAPs) in *Arabidopsis* to identify the phytoplasma effector that induces these virescence and phyllody symptoms (hereafter leafy flower). Large-scale screening revealed SAP54 to be the effector causing leafy flower and crinkled silique phenotypes in *Arabidopsis* [2]. Furthermore, the PHYL1 effector of Onion yellows phytoplasma, an effector orthologous to SAP54, also results in a leafy flower phenotype in *Arabidopsis* expressing the *PHYL1* gene [3], suggesting that SAP54 and PHYL1 play roles in leafy flower formation. Our previous study indicated that Peanut witches'-broom (PnWB) phytoplasma also occurs leafy flower symptoms in *Catharanthus roseus* plants [4], and its *PHYL1* gene has also been identified [5]. To evaluate the PHYL1 of PnWB function, the gain-of-function study in *Arabidopsis* plants is an approach to study the mechanism of leafy flower development. However, the transgenic *Arabidopsis* expressing *SAP54* (*SAP54* plants) have a seedless problem that restricted the further study in function of effectors. Therefore, an alternative strategy for *PHYL1/SAP54* gain-of-function *in vivo* that is independent from the transgenic approach is needed.

Since the 1990s, plant viral vectors have been developed to carry foreign genes for different purposes. Unlike the transgenic approach, a viral vector has several advantages, such as self-replication and long-distance movement, allowing the systemic spread of interesting foreign sequences for efficient expression or virus-induced gene silencing (VIGS) in plant [6–12]. A viral suppressor is a key regulator for counteracting the RNA-silencing defense in plants [13–15]. Because of silencing suppression, foreign proteins in viral vector-infected plants are expressed to a higher degree than in transgenic plants [16–18]. In addition, the viral suppressor interferes microRNA (miRNA) biogenesis, resulting in severe symptoms that affect the normal growth status of host plants [19, 20]. To overcome this issue, a deconstructed vector was applied for over-expression of a foreign gene through the expression of the required viral elements [21, 22]. Moreover, this deconstructed vector can also overcome the problems of size limitations and the deletion of foreign genes, which occurred with viral vectors [21].

Tobacco rattle virus (TRV) and *Potato virus X* (PVX), which has a weak suppressor in silencing suppression, have been widely applied for VIGS in loss-of-function studies [12]. A suitable viral vector, other than a VIGS vector, for rapid gain-of-function studies in infected wild-type or mutant plants is also important; especially when the transgene causes a lethal phenotype in seedlings of the next generation. Many reports have demonstrated that several virus species can express *green fluorescent protein* (*GFP*) gene for proving of the concept in viral vector development; however, functional study of gene is lacking [6, 23].

The attenuated *Turnip mosaic virus* (TuMV) strain (TuGK) has an Arg182Lys mutation in helper component-proteinase (HC-Pro^{R182K}). HC-Pro^{R182K} is a mutant of a gene-silencing suppressor that has lost its ability to suppress the miRNA pathway, results in no symptoms in TuGK-infected *Arabidopsis thaliana* (hereafter *Arabidopsis*) and *Nicotiana benthamiana* plants [19, 24]. TuGK has been modified as a viral vector to express *GFP* for indicating and monitoring the virus location in the host [19]. An infectious, full-length cDNA clone of TuGK has been constructed in the mini binary vector pBD003 to generate pBD-TuGK, which can be directly inoculated into host plants via agro-infiltration to induce an initial infection [24]. TuGK-infected *Arabidopsis* plants is symptomless [19], making TuGK suitable for the over-expression of foreign genes in *Arabidopsis* plants, with few or no side effects due to the severe pathogenicity of the virus.

In this study, TuGK was used as a viral vector for rapid expression to study the function of the *PHYL1* and *SAP54* gene in *Arabidopsis* plants. Recombinant TuGK viruses could

successfully express effectors in Arabidopsis and mimic the leafy flower phenotype of the transgenic plants, demonstrating the use of TuGK as a rapid system for gain-of-function studies *in planta*.

Materials and Methods

Plant materials and growth conditions

Arabidopsis seeds were surface sterilized and chilled at 4°C for 2 days before being sown on Murashige and Skoog (MS) medium with/without suitable antibiotics for selection. One-week-old seedlings that had germinated on the MS plates were transferred to soil. *N. benthamiana* seeds were sown in soil. All of the seedlings and plants were maintained in either a growth chamber or greenhouse (16 hr light/8 hr dark, 20 to 25°C).

Construction of effector genes in the TuGK viral vector and virus infection

The *PHYLL1* gene was amplified from cDNA extracted from PnWB-infected *C. roseus* plants by reverse transcription-polymerase chain reaction (RT-PCR) using the primers PnHeI-SAP54 (PnWB) (5' -CAAGGCTAGCATGGATCCAAAACCTCCAGAA-3') and MSAP54-NheI (PnWB) (5' -CACAGCTAGCGTTTTTTTTTCATCATTTAAATC-3'), which contains *NheI* sites (underlined). The gene was then inserted into the pGEM-T easy vector (Promega) to generate pGEM-PHYLL1. The *SAP54* gene of AYWB was amplified from pDONR207-SAP54 (provided by Dr. Saskia Hogenhout) using the primers PSAP54-NheI (5' -GTACAAGGCTAGCATGGA TAAAGATATTGCAAGCACT-3') and MSAP54-NheI (5' -AAACACAGCTAGCATTATTTT CATCATTTAA-3'), which contains *NheI* sites (underlined). The *SAP54* and *PHYLL1* genes were inserted into the pBD-TuGK viral vector [24] via *NheI* digestion and ligation to generate pBD-TuGK-SAP54 and pBD-TuGK-PHYLL1.

The infectious viral clones were transformed into the *Agrobacterium tumefaciens* C58C1 strain, and virus infection was performed in *N. benthamiana* plants using the agro-infiltration procedure [24]. Four days after infiltration, the infiltrated leaves of *N. benthamiana* plants were collected to analyze viral infectivity and were used as the primary inoculum to mechanically inoculate Arabidopsis plants. Recombinant TuGK infection was performed in 2.5-week-old Col-0 or *dcl2-4/dcl4-1* double-mutant (*dcl2/4*) plants. Flower tissues from plants at 20 days post-inoculation (dpi) were used for gene profile evaluation.

Longitudinal sectioning of shoot apical meristem and confocal microscopy

The shoot apical meristem (SAM) of 4 dpi TuGK- or TuGK-PHYLL1-infected Arabidopsis and *N. benthamiana* plants were embedded in 5% agar and sectioned at 200- μ m thickness using a microslicer (DTK-1000; Dosaka EM, Japan). The GFP fluorescence in the SAM was monitored using a Leica TCS SP5 II confocal laser-scanning microscope (Joint Center for Instruments and Researches, College of Bioresources and Agriculture, National Taiwan University) that was equipped with a multiline argon laser with a filter set for GFP fluorescence [excitation filter Acousto-optic Tunable filter 488, emission bandwidth 502 to 572 nm, PMT2 offset (-1.0)/gain (895.3)] and a filter set for chlorophyll fluorescence [excitation filter Acousto-optic Tunable filter 488, emission bandwidth 608 to 677 nm, PMT3 offset (0.0)/gain (855)]. All images were graphically arranged using Adobe Photoshop CS3 software (Adobe Systems Inc., Mountain View, CA, U.S.A.).

Transgenic Arabidopsis expressing *PHYL1*

The *PHYL1* gene was amplified from pGEM-PHYL1 with the primers FG-PHYL1-Pn (5' -CA CCATGGATCCAAAACCTTCCAGAACTAGTAGCAG-3') and RG-PHYL1-Pn (5' -TTAGT TTTTTTCATCATTTAAATCATTTAA-3'). The PCR fragment was cloned into the pENTR/D-TOPO vector (Invitrogen) according to the manufacturer's instructions to generate pENTR-PHYL1. The Gateway system was used to transfer the *PHYL1* gene to the pBA-DC-myc binary vector [25], generating pBA-PHYL1. The binary plasmid was transformed into the *Agrobacterium tumefaciens* ABI strain for transgenic Arabidopsis transformation using the floral-dip procedure [26]. The transformant lines were screened on MS medium containing 10 µg/ml Basta (Sigma).

PHYL1 and SAP54 antiserum production

To express recombinant PHYL1 protein in *E. coli*, the gene was amplified from pGEM-PHYL1 using the primers PPn-NheI (5' -TATGGCTAGCATGGATCCAAAACCTTCCAGA-3') and MPn-XhoI (5' -GGTGCTCGAGGTTTTTTTCATCATTTAAAT-3'), which contain *NheI* and *XhoI* sites (underlined). To express the recombinant SAP54 protein in *E. coli*, the gene was amplified from pDONR207-SAP54 using the primers PAY-NheI (5' -TATGGCTAGCATGGATAAAGA TATTGCAAG-3') and MAY-XhoI (5' -GGTGCTCGAGATTATTTTCATCATTTAAAG-3'), which contain *NheI* and *XhoI* sites (underlined). The PCR fragments were digested with *NheI*/*XhoI* and ligated into pET28a (Novagen) that had been digested with the same restriction enzymes to generate pET-PHYL1 and pET-SAP54.

E. coli cells transformed with either pET-PHYL1 or pET-SAP54 were individually cultured in 500 ml of LB medium at 37°C until the absorbance at 600 nm reached 0.5. After that, the 0.5 mM isopropyl-D-1-thiogalactopyranoside (IPTG) was added in the culture and grown at 20°C for 6 hr. Recombinant protein purification and antiserum production were performed using modified protocols published by Chiu et al [27]. Approximately 1 mg of either recombinant PHYL1 or SAP54 protein was mixed with Freund's adjuvant (1:1 v/v) and injected into a New Zealand white rabbit once per week; the procedure was repeated 4 times. For the first injection, the "complete" adjuvant was used, and the "incomplete" adjuvant was for the subsequent injections. The titer of the antiserum was analyzed using western blotting. Institutional Animal Care and Use Committee (IACUC) of National Taiwan University (NTU) approved the antiserum production in this study. The feeding and care of the experimental rabbits were bred at animal room of Institute of Biotechnology of NTU. All antiserum processing, including animal welfare, ameliorates suffering, and sacrifice, were performed according to institutional guidelines under the regulation of the IACUC of NTU and to laws of Taiwan on animal protection.

Western blot analysis

Plant tissue was ground in 5–10 volumes (w/v) of 20 mM phosphate buffer, pH 7.0, and the plant extracts were suspended in 2 volumes (w/v) of 2× protein sample dye (2% SDS, 10% glycerol, 1% β-mercaptoethanol, 0.005% bromophenol blue, and 50 mM Tris-HCl, pH 6.8), denatured 100°C for 10 min and then cooled on ice for 2 min. The protein samples were separated on 12% polyacrylamide-SDS gels and then transferred to a PVDF membrane (GE Healthcare) with transfer buffer (50 mM Tris-HCl, 40 mM glycine, 1 mM SDS, and 20% methanol). For TuMV coat protein (CP) detection, the CP antiserum was used at a 10,000× dilution (Chiu et al., 2013). For phytoplasma effector detection, SAP54 or PHYL1 antisera were used at a 10,000× dilution. For GFP detection, a GFP monoclonal antibody (GE Healthcare) was used at an 8000× dilution. HRP-conjugated anti-rabbit or anti-mouse antibodies (GE Healthcare) were used as secondary antibodies at a 10,000× dilution, and the signals were detected using

WesternBright ECL (Advansta). The membrane was stained with staining solution (0.6 mM Coomassie blue R-250, 50% methanol, 10% acetic acid) to perform ribulose-1,5-bisphosphate carboxylase (RUBISCO) staining as a loading control.

Identification of flower-related gene expression in *SAP54* plants

Total RNA was extracted from normal flowers of Col-0 plants or leafy flowers of *SAP54* plants using TRIzol reagent (Invitrogen) according to the manufacturer's protocol. One sample for each condition was used for the NGS data. The whole-transcriptome profiles of the Col-0 and *SAP54* plants were analyzed using an Illumina HiSeq 2000 (Genomics BioSci & Tech Co.). The raw transcriptome reads of Col-0 and *SAP54* plants are available in the NCBI Short Read Archive under accession number SRR1979100 (normal flower of Col-0 plant), and SRR1979105 (leafy flower of *SAP54* plant). The flower-related gene expression profiles were identified from the whole-transcriptome profiles. The raw reads for the *AtAP3* (AT3G54340), *AtSVP* (AT2G22540), *AtFT* (AT1G65480), and *AtUBQ10* (AT4G05320) genes from Col-0 and *SAP54* flower tissues were used to calculate the reads per kilobase per million mapped reads (RPKM) values of the 3 flower-related genes using the CLC Genomics Workbench 7.5.1 (CLC bio).

Real-time RT-PCR

Total RNA was extracted from 0.1 g of plant tissue using the Trizol reagent (Invitrogen). RT was performed using the SuperScript III first-strand synthesis system (Invitrogen) following the manufacturer's instructions. Real-time PCR was performed using a LightCycler 480 instrument (Roche) with four sets of primers: PAP3 (5' -GAGTGTGGACGAGCTTGA-3') and MAP3 (5' -TTCTTGGTGGTCTCGATCTG-3') for the amplification of the *AtAP3* gene; PSVP (5' -GGAATGCAATTGATGGATGA-3') and MSVP (5' -TCCTTCCTCGTACACAGCAG-3') for the amplification of the *AtSVP* gene; PFT (5' -CCTTTGGCAATGAGATTGTG-3') and MFT (5' -GCCAAGCTGTGCAAACAATA-3') for the amplification of the *AtFT* gene; and PUBQ10 (5' -CACTTCACTTGGTCTTGCCT-3') and MUBQ10 (5' -TATCCTGGATCTTGGCCTTC-3') for the amplification of the *AtUBQ10* gene. The *AtAP3*, *AtSVP*, *AtFT*, and *AtUBQ10* transcripts were quantified via a relative cycle threshold (Ct) method. All experiments were performed in triplicate to compensate for possible loading errors. The relative expression levels were calculated based on the $\Delta\Delta C_t$ value, and each sample was normalized according to the expression levels of *AtUBQ10*.

Results

TuGK expresses phytoplasma effectors *in planta*

pBD-TuGK was used to carry the *PHYL1* or *SAP54* gene (Fig 1A). Both effector genes were fused at the C-terminus of GFP and inserted between the *Nib* and *CP* genes with N1a protease cleavage sites (Fig 1A). pBD-TuGK-PHYL1 and pBD-TuGK-SAP54 were produced by the TuGK-PHYL1 and TuGK-SAP54 recombinant viruses in *N. benthamiana* plants after agro-infiltration and exhibited a GFP signal under fluorescence microscopy (Fig 1B). Compared with plants infected with a wild-type TuMV that expresses GFP (TuGR), GFP fluorescence was lower in the TuGK-, TuGK-PHYL1-, and TuGK-SAP54-infected plants (Fig 1B). Thus, TuGK can express both effectors at lower expression levels.

Evaluating the efficiency of PHYL1 and SAP54 expression by TuGK

TuGR and TuGK expressed GFP in both inoculated leaves (ILs) and systemic leaves (SLs) of *N. benthamiana* plants at 4 dpi (Fig 2A). In contrast, only ILs showed TuGK-PHYL1 and

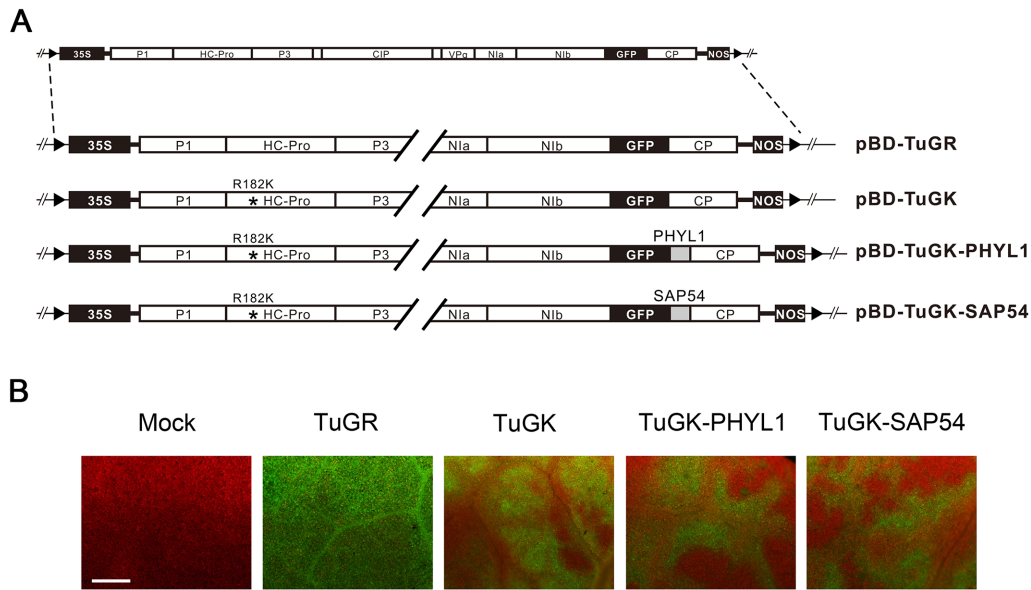


Fig 1. Recombinant TuGK viral vectors expressing phytoplasma effector genes in *Nicotiana benthamiana* plants. A, Schematic diagram of pBD-TuGR, pBD-TuGK, pBD-TuGK-PHYL1, and pBD-TuGK-SAP54. The TuMV genes are indicated by white boxes. The *green fluorescent protein* gene (*GFP*) is indicated by a black box. The *SAP54* of AYWB and *PHYL1* of PnWB genes are indicated by gray boxes. Asterisks (*) indicate the Arg182Lys mutation (R182K) in HC-Pro. The 35S promoter and NOS terminator are indicated by black boxes. The left border (LB) and right border (RB) sequences are indicated. B, Viral infectivity assay of the recombinant viruses. GFP expression by TuGR, TuGK, TuGK-PHYL1, and TuGK-SAP54 in *N. benthamiana* plants. Images were acquired of *N. benthamiana* plants at 4 dpi with fluorescence microscopy at 400x magnification. Bar, 25 μ m.

doi:10.1371/journal.pone.0130139.g001

TuGK-SAP54 infection at 4 dpi (Fig 2A), suggesting that phytoplasma effectors might interfere with TuGK replication and infection in host plants. Surprisingly, the *PHYL1* gene was deleted from the TuGK genome in SLs, leaving only GFP (25 kDa) and truncated fusion proteins in SLs at 8 dpi (Fig 2B). Note, the *SAP54* gene was also deleted from TuGK in some instances (data not shown).

TuGK-infected leaves of *N. benthamiana* plants at 4 dpi were used as the inoculum to inoculate Arabidopsis plants. TuGK-PHYL1- and TuGK-SAP54-infected Col-0 plants showed partial deletion of the GFP-PHYL1 and GFP-SAP54 fusion proteins at 20 dpi; nevertheless, high levels of the fusion proteins persisted (Fig 2C). Moreover, SAP54 and PHYL1 antisera specifically detected GFP-SAP54 and GFP-PHYL1, respectively, in the infected Arabidopsis plants (Fig 2D), suggesting that TuGK expresses either the *PHYL1* or *SAP54* effector gene, respectively. Although PHYL1 and SAP54 exhibit 60.4% similarity, no cross-reactivity was observed by western blotting, demonstrating the high specificity of the antisera in distinguishing these two effectors.

TuGK was detected in SAM

The SAM is an important position in plants with regard to leafy or flower organ determination. We assume that 35S promoter-driven effectors affect the gene expression in the SAM of *PHYL1* and *SAP54* plants, resulting in leafy flowers. Next, we evaluated whether TuGK can migrate to the SAM and express the effector in the meristem. The results of longitudinal section showed GFP fluorescence in the SAM regions of TuGK- and TuGK-PHYL1-infected *N. benthamiana* plants (Fig 3). Moreover, the SAM of Arabidopsis also showed GFP fluorescence of TuGK (S1 Fig). These results indicated that TuGK and TuGK-PHYL1 migrate to the meristem and express GFP-PHYL1 in the SAM region. Therefore, TuGK-delivered PHYL1 might affect gene expressions in the meristem as in *PHYL1* plants.

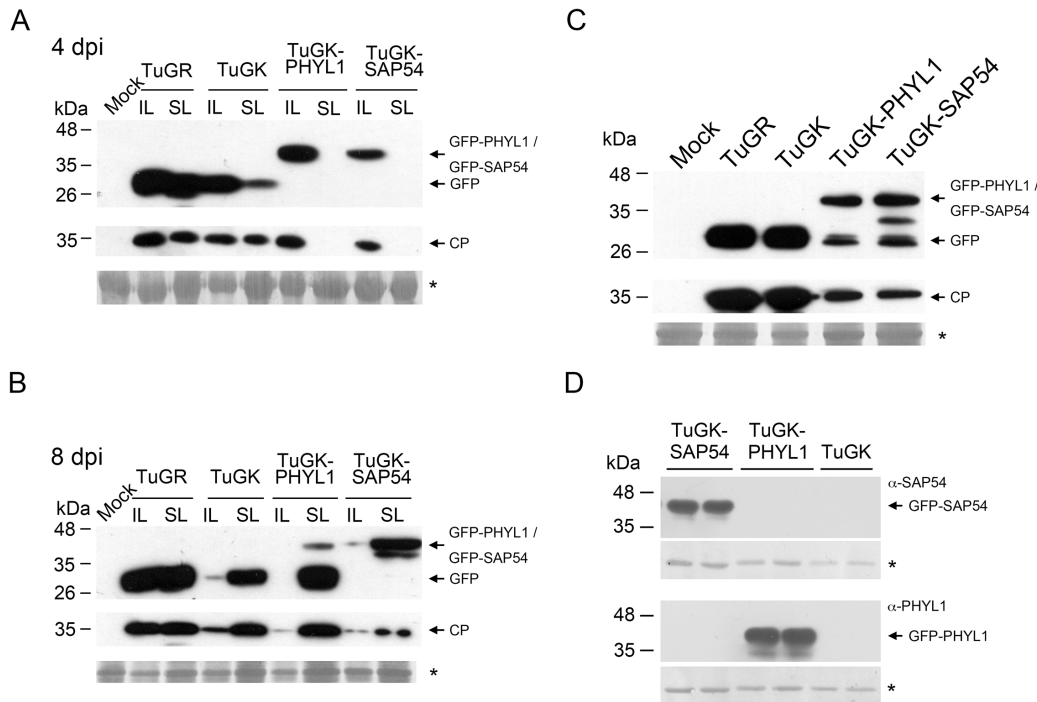


Fig 2. Detection of effector expression in TuGK-PHYL1- and TuGK-SAP54-infected plants. Foreign gene expression in TuMV-infected *Nicotiana benthamiana* plants at 4 dpi (A) or 8 dpi (B). IL indicates an inoculated leaf, and SL indicates a systemic leaf. C, Foreign gene expression in TuMV-infected *Arabidopsis dcl2-4/dcl4-1* double-mutants (*dcl2/4*). TuGR, a wild-type TuMV that expresses the *green fluorescent protein (GFP)* gene; TuGK, an HC-Pro Arg182Lys mutant of TuMV that expresses the *GFP* gene; TuGK-PHYL1, TuGK expressing the *GFP-PHYL1* fusion gene; TuGK-SAP54, TuGK expressing the *GFP-SAP54* fusion gene. The upper panels were detected using an 8,000× dilution of the GFP antibody. The lower panels were detected using a 10,000× dilution of TuMV coat protein (CP) antiserum. D, SAP54 and PHYL1 detection using specific antisera at 10,000× dilutions. The large subunit of ribulose-1,5-bisphosphate carboxylase (*) was used as a loading control.

doi:10.1371/journal.pone.0130139.g002

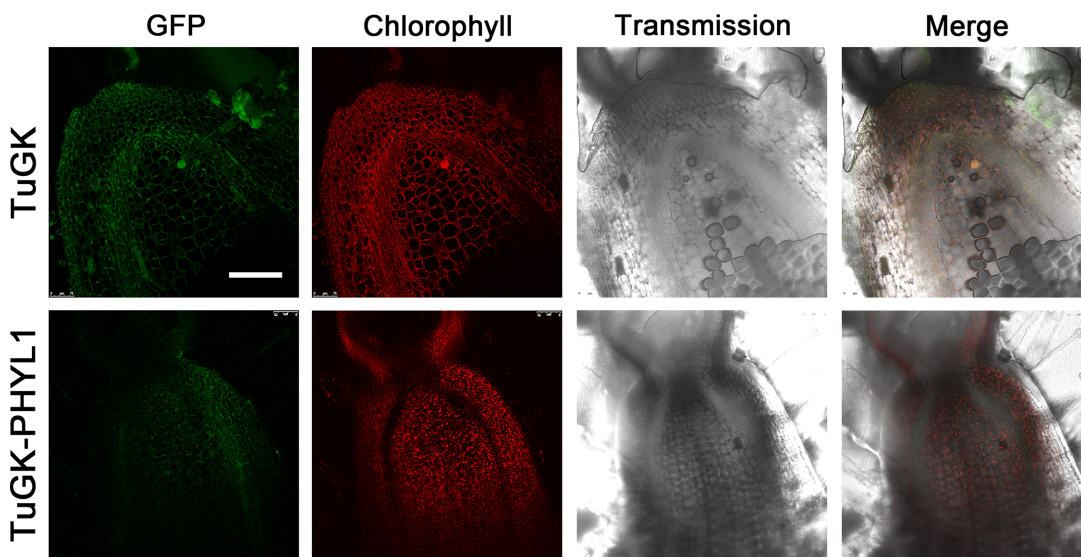


Fig 3. Longitudinal section of the shoot apical meristem (SAM) of *Nicotiana benthamiana* plants. The TuGK- and TuGK-PHYL1-infected SAM sections were evaluated by confocal microscopy. Complete stacks demonstrate that GFP (green), GFP-PHYL1 (green) and chlorophyll (red) were present in the SAM region. The SAM tissues were corrected at 4 dpi of TuGK- or TuGK-PHYL1-infected plants. Bar, 100 μm.

doi:10.1371/journal.pone.0130139.g003

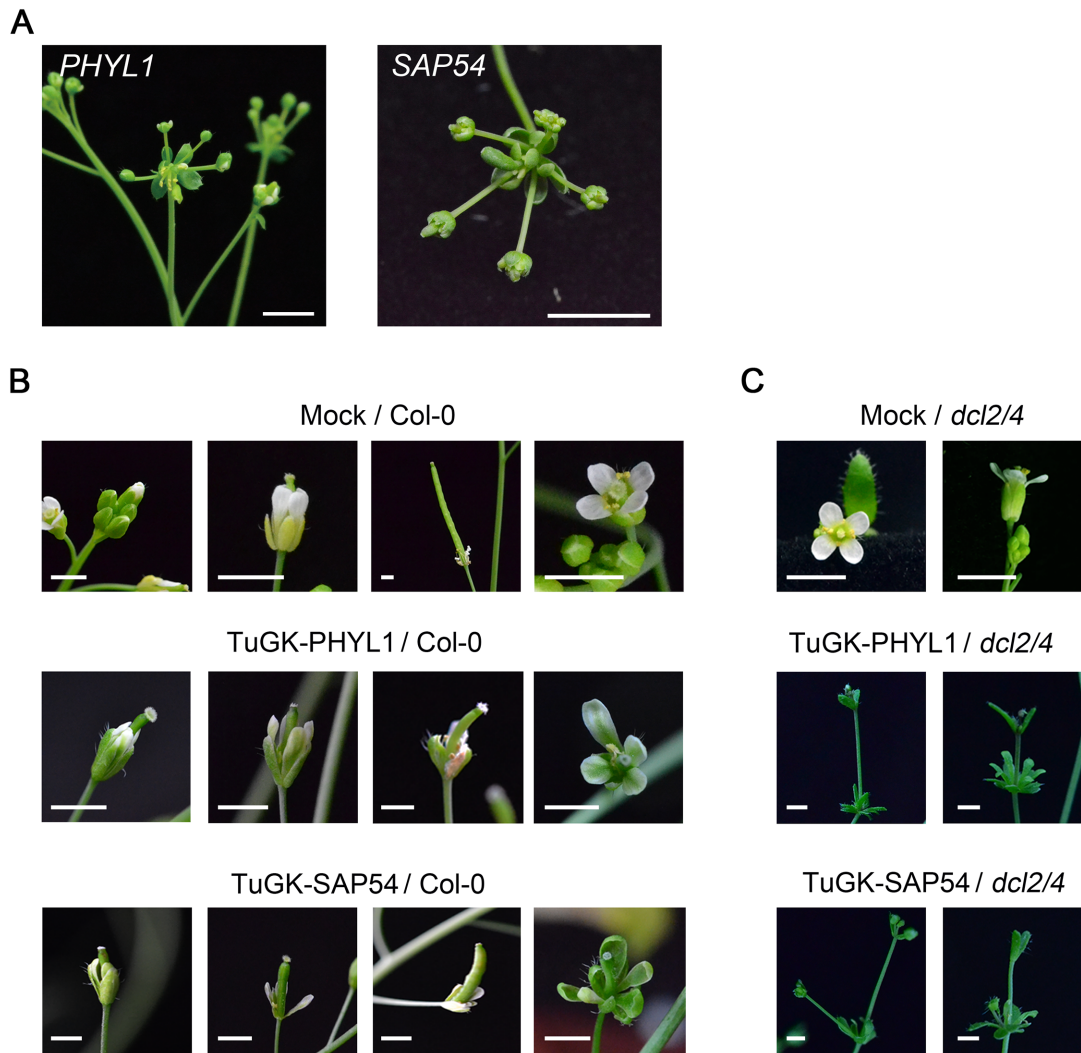


Fig 4. Leafy flower phenotypes of TuGK-PHYL1- and TuGK-SAP54-infected Arabidopsis plants. A, The leafy flower phenotypes of *SAP54* and *PHYL1* plants. Bar, 0.2 cm. The leafy flower phenotypes of TuGK-SAP54- or TuGK-PHYL1-infected Col-0 (B) and *dcl2/4* (C) plants. Mock indicates inoculation with buffer alone. The photographs were taken at 20 dpi. Bar, 0.2 cm.

doi:10.1371/journal.pone.0130139.g004

Recombinant TuGK-PHYL1 and TuGK-SAP54 trigger leafy flower phenotypes in infected Arabidopsis

SAP54 plants (kindly provided by Dr. Hogenhout) display a leafy flower phenotype (Fig 4A) [2], indicating that the *SAP54* effector plays an important role in controlling phyllody symptoms in phytoplasma-infected plants. Moreover, our data showed a leafy flower phenotype for transgenic Arabidopsis expressing *PHYL1* (Fig 4A), suggesting that both effectors exert an identical function. To test whether TuHG-PHYL1 and TuGK-SAP54 can trigger the leafy flower phenotype, both recombinant viruses were infected into Arabidopsis plants. At 20 dpi, leafy flowers were observed in the TuGK-PHYL1- and TuGK-SAP54-infected Col-0 plants, whereas the mock-infected Col-0 plants showed normal flowers (Fig 4B). In addition, the *dcl2/4* plant is a double mutant in *Dicer-like 2* (*DCL2*) and *Dicer-like 4* (*DCL4*) genes, which is more susceptible to TuGK infection [19]. The TuGK-PHYL1- and TuGK-SAP54-infected *dcl2/4* plants also showed leafy flowers (Fig 4C). Neither TuGK-PHYL1 nor TuGK-SAP54 resulted in severe

Table 1. Comparison of the leafy flower rate between transgenic plants and recombinant TuGK-infected plants.

	Phenotype		Total plants	Prop. ^c	(%)	p-value ^d
	Leaf flower ^a	Normal flower ^b				
<i>PHYL1</i> plant ^e	46	728	774		5.9	NA
TuGK- <i>PHYL1</i> ^f /Col-0	11	48	59		18.6	2×E-4
TuGK- <i>PHYL1</i> / <i>dcl2/4</i>	15	44	59		25.4	3.1×E-8
TuGK-SAP54/Col-0	5	10	15		33.3	1.9×E-5
TuGK-SAP54/ <i>dcl2/4</i>	2	11	13		15.4	0.16

^aThe number of plants showing the leafy flower phenotype.

^bThe number of plants showing the normal flower phenotype.

^cThe proportions of the leafy-flower plants.

^dThe p-value of Chi-squared test.

^eTransgenic Arabidopsis expressing the *PHYL1* gene.

^fArabidopsis plants infected with TuGK-*PHYL1* or TuGK-SAP54.

doi:10.1371/journal.pone.0130139.t001

symptoms in Col-0 or *dcl2/4* plants (Fig 4B and 4C). These results suggested that TuGK delivers these effectors to SAM and trigger leafy flower.

The TuGK vector enhances the phenotype formation rate

In *PHYL1* plants, the *PHYL1* gene was constructed under the control of the 35S promoter in the pBA-DC-myc binary vector and was transferred into Arabidopsis for over-expression. The T0 lines of the *PHYL1* plants showed a low ratio of leafy flower formation. Of the 774 individual T0 seedlings of *PHYL1* plants, which all showed Basta resistance (a selection marker), only 46 showed a leafy flower phenotype (Table 1). In this case, the leafy flower formation rate is 5.9% in this transgenic approach (Table 1). A similar phenomenon was also observed in the T0 seedlings of *SAP54* plants (data not shown), suggesting the existence of unclear mechanism(s) influence the effector-mediated leafy flower formation.

The leafy flower rates were 18.6% and 25.4% in TuGK-*PHYL1*-infected Col-0 and *dcl2/4* plants, respectively, 3 to 5 times the ratio compared with the transgenic approach (Table 1). Similarly, leafy flower rates of 15.4 to 33.3% were found for TuGK-SAP54-infected Arabidopsis (Table 1). These data indicated that the *PHYL1*- and *SAP54*-mediated leafy flower formation rate could be enhanced through the TuGK expression approach. Moreover, the DCL2/DCL4-dependent virus defense system might interfere with recombinant virus infection and result in a reduction in the expression of foreign genes [19]. Despite the results of TuGK-SAP54 infection, TuGK-*PHYL1* triggered a leafy flower formation rate in *dcl2/4* plants of 25.4%, whereas a formation rate of 18.6% was observed for TuGK-*PHYL1*-infected Col-0 plants (Table 1), suggesting that TuGK-expressed *PHYL1* in *dcl2/4* plants can also enhance the phenotype formation.

Flower-related gene expression profiles in TuGK-*PHYL1*- and TuGK-SAP54-infected leafy flowers

To compare the gene expression profiles of Col-0 and *SAP54* plants, we evaluated the expression levels of 3 flower-related genes (*AtAP3*, *AtSVP*, and *AtFT*) in flower tissues from Col-0 and *SAP54* plants based on their transcriptome profiles (Fig 5). The *AtAP3* and *AtFT* genes, which promote flowering, were down-regulated in *SAP54* plants, whereas the flowering repressor *AtSVP* was up-regulated (Fig 5).

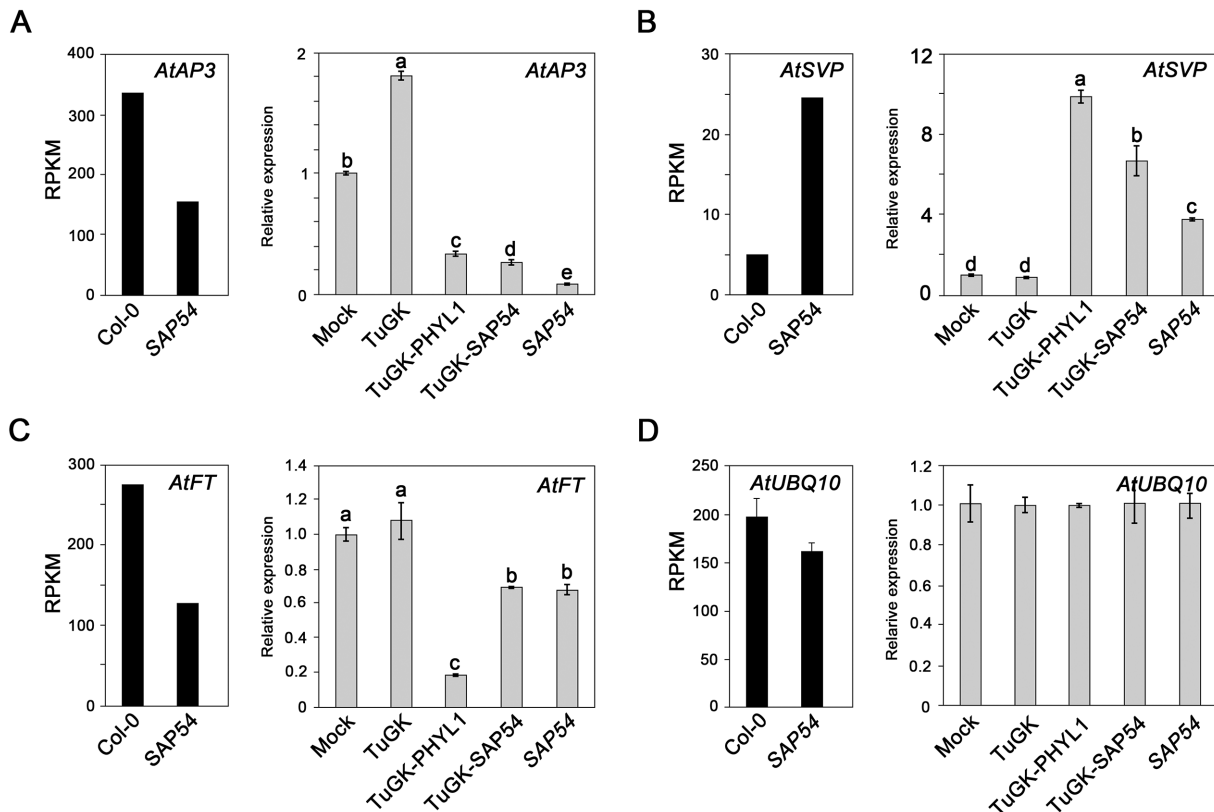


Fig 5. Flower-related gene expression in TuGK-PHYL1- and TuGK-SAP54-infected Arabidopsis flower tissues. The expression profiles of the *AtAP3* (A, left panel), *AtSVP* (B, left panel), *AtFT* (C, left panel), and *AtUBQ10* (D, left panel) genes in flower-tissues of Col-0 and *SAP54* plants were evaluated by transcriptome deep sequencing. The reads per kilobase per million mapped reads (RPKM) values are used to indicate gene expression levels. The bars represent the SE of 6 *AtUBQ10* isoforms ($n = 6$). Real-time RT-PCR evaluation of *AtAP3* (A, right panel), *AtSVP* (B, right panel), *AtFT* (C, right panel), and *AtUBQ10* (D, right panel) expression in various recombinant TuGK virus-infected *dcl2-4/dcl4-1* (*dcl2/4*) plants at 20 dpi. *SAP54* represents *SAP54* plants. The bars represent the SE ($n = 3$). The relative expression levels were normalized to the *AtUBQ10* level. The letters indicate significant differences among these relative expression levels of the RNA samples tested by Fisher's least significant difference (LSD) method at 'alpha' = 0.05, with false discovery rate (FDR) correction after an analysis of variance (ANOVA).

doi:10.1371/journal.pone.0130139.g005

Next, real-time PCR was used to evaluate *AtAP3*, *AtSVP*, and *AtFT* expression levels in TuGK-PHYL1- and TuGK-SAP54-infected Arabidopsis (Fig 5). *AtUBQ10* is a housekeeping gene that has been used as a references gene for real-time RT-PCR normalization in many studies [28–30]. *AtUBQ10* has 6 alternative splicing isoforms (S1 Table), and the transcriptome profile indicated no significant differences of the average RPKM of 6 isoforms (p -value of t-test is 0.314) between Col-0 and *SAP54* plants (Fig 5D, left panel). Moreover, the real-time RT-PCR primer set for *AtUBQ10* was designed based on the conserved region of the 6 isoforms, and the real-time RT-PCR results indicated that *AtUBQ10* expression levels are consistent in virus-infected or uninfected Arabidopsis plants (Fig 5D, right panel). These results indicated that *AtUBQ10* expression is stable under the various conditions and treatments in this study and that it can be used as a references gene for normalization of flower-related gene expression.

The expression levels of *AtAP3* and *AtFT* were repressed in TuGK-PHYL1-infected or TuGK-SAP54-infected Arabidopsis and *SAP54* plants compared to mock-infected plants, whereas *AtSVP* was up-regulated in these plants (Fig 5A, 5B and 5C; right panels). These real-time RT-PCR results are consistent with the deep sequencing results, indicating that the TuGK expression system is consistent with the transgenic approach.

Discussion

The lack of symptoms of TuGK-infected plants is helpful for phenotype observation

Foreign gene expression by viral vectors *in planta* has an advantage in shortening the development time compared with transgenic plants. However, most viral vectors are constructed from viral strains that cause severe symptoms and affect the normal growth status of the plant host. Thus, it can be difficult to distinguish whether the phenotypes are caused by the expressed gene or plant immune responses. A deconstructed vector approach utilizes the minimum required viral elements for efficient expression; the missing functions can be provided by non-viral components to avoid symptoms. The deconstructed approach thus provides a solution for the symptom issue; however, the vector delivery system still relies on the agrobacterium-mediated transgenic method.

The HC-Pro^{R182K} of TuGK is a mutant defective in miRNA pathway suppression, resulting in a lack of symptoms in infected plants [19]. Therefore, TuGK can be used to perform unambiguous gain-of-function analyses in infected plants. Currently, the high-throughput next-generation (NGS) technique provides a powerful method to analyze whole-transcriptome profiles. Hundreds to thousands of candidate genes can be identified via high-throughput network analysis [4], and an efficient way to verify the functions of these candidate genes is needed. The TRV vector with the Gateway recombinant system has been developed for efficiency in constructing VIGS sequences of interests [12]. Therefore, the Gateway cassette can be employed with the TuGK vector for future high-throughput gain-of-function analyses.

The stability of a heterologous gene in a viral vector is dependent on whether the gene interferes with the viral infection pathway. In addition, losing the foreign gene is strongly dependent on demographic conditions [31]. For instance, the *GFP* gene is more stable in the short-term passages of TuMV, whereas the losing *GFP* gene in the long-term passage [31]. We assume the PHYLL1 and SAP54 effectors might cause side effect to interfere with TuMV infection, whereas the harmless *GFP* gene can be passed to many progenies by viral vectors [10].

TuGK can deliver effectors to the meristem and trigger leafy flower development

It is generally considered that the meristem of a plant is a cell division-active and virus-free region [32]. However, recent studies have demonstrated that several viruses, including *Tobacco ringspot virus*, *Pepper ringspot virus*, *PVX*, *Odontoglossum ringspot virus*, and *Barley stripe mosaic virus*, can infect the meristem region [32–37]. The confocal section data indicated that TuMV migrates to the meristem, suggesting that a TuGK-delivered foreign gene can affect host gene regulation in the meristem, resulting in altered morphology. Indeed, TuGK-PHYLL1- or TuGK-SAP54-infected *Arabidopsis* showed a leafy flower phenotype identical to *PHYLL1* and *SAP54* plants.

Our previous study demonstrated that PnWB-mediated leafy flowers in *C. roseus* plants, which show up-regulation of *CrSVP1* and *CrSVP2*, but down-regulation of *CrAP3.1*, *CrAP3.2*, and *CrFT* [4]. The gene expression profiles in TuGK-PHYLL1- and TuGK-SAP54-infected *Arabidopsis* plants indicated that *AtAPI*, *AtSVP*, and *AtFT* expressions are consistent as transgenic *Arabidopsis* and PnWB-infected *C. roseus* plants. Therefore, these data indicated that the TuGK vector can be used for gain-of-function studies. Moreover, the T0 lines of *PHYLL1* and *SAP54* plants showed severe leafy flowers that did not produce seeds. TuGK-PHYLL1 and TuGK-SAP54 infection of *Arabidopsis* provides sufficient experimental material and can infect various mutant plants for further genetic analysis.

Furthermore, based on these data, we can immediately ask whether the *PHYLL1* or *SAP54* effector acts similarly to the HC-Pro in silencing suppression or compensate the loss-of-miRNA suppression of HC-Pro^{R182K}. Different pathogen effectors have been shown to exhibit synergistic effects upon co-infection [38]. However, TuGK-*PHYLL1*- and TuGK-*SAP54*-infected Arabidopsis plants did not exhibit the severe yellow mosaic symptoms of TuMV, indicating that *PHYLL1* and *SAP54* did not compensate for the loss-of-function of HC-Pro^{R182K}.

The TuGK vector enhances the phenotype formation rate

The leafy flower formation rate of the T0 lines of *PHYLL1* plants was 5.9% (Table 1) and a similar phenomenon was also observed for *SAP54* plants (data not shown). Most of Basta-resistant T0 lines of *PHYLL1* or *SAP54* plants produced normal flowers. We assume that the protein stability or another unclear mechanism affects *PHYLL1*- or *SAP54*-mediated leafy flower formation. However, the phenotype formation rate of the TuGK-*PHYLL1*- or TuGK-*SAP54*-infected plants was increased by 2.6 to 5.6 times compared with the *PHYLL1* or *SAP54* plants. These data indicated that the TuGK vector enhances the phenotype formation.

Conclusions

In this study, we used the TuGK mild strain, which lacks the ability to suppress the miRNA pathway, as a vector for a gain-of-function study and found phenotypes and gene expression levels similar to those of transgenic plants. Moreover, the TuGK expression system serves as an additional strategy for effector expression to bypass the issue of lack of seeds with *PHYLL1* and *SAP54* plants. Combination of the Gateway recombinant system with the TuGK vector will facilitate future cloning and efficient screening in gain-of-function studies.

Supporting Information

S1 Fig. Longitudinal section of the shoot apical meristem (SAM) of Arabidopsis plants.

The mock- and TuGK-infected SAM sections were evaluated by confocal microscopy. Complete stacks demonstrate that GFP (green), and chlorophyll (red) were present in the SAM region. The SAM tissues (white dashed-line boxes) were corrected at 7 dpi of mock- or TuGK-infected Arabidopsis plants. Bar, 200 μm .

(TIF)

S1 Table. The read counts and RPKM of 6 *AtUBQ10* isoforms in Col-0 and *SAP54* plants.

(DOCX)

Acknowledgments

We thank Dr. Saskia Hogenhout for providing the transgenic *SAP54* Arabidopsis seeds and the pDONR207-*SAP54* plasmid.

Author Contributions

Conceived and designed the experiments: SSL CPL HFL. Performed the experiments: SFH YHH SFH CYY WYC TYT. Analyzed the data: SFH LYDL SSL. Contributed reagents/materials/analysis tools: CPL HFL. Wrote the paper: SSL.

References

1. Bai X, Correa VR, Toruño TY, Ammar e-D, Kamoun S, Hogenhout SA. AY-WB phytoplasma secretes a protein that targets plant cell nuclei. *Mol Plant Microbe Interact*. 2009; 22: 18–30. doi: [10.1094/MPMI-22-1-0018](https://doi.org/10.1094/MPMI-22-1-0018) PMID: [19061399](https://pubmed.ncbi.nlm.nih.gov/19061399/)

2. MacLean AM, Sugio A, Makarova OV, Findlay KC, Grieve VM, Tóth R, et al. Phytoplasma effector SAP54 induces indeterminate leaf-like flower development in Arabidopsis plants. *Plant Physiol.* 2011; 157: 831–841. doi: [10.1104/pp.111.181586](https://doi.org/10.1104/pp.111.181586) PMID: [21849514](https://pubmed.ncbi.nlm.nih.gov/21849514/)
3. Maejima K, Iwai R, Himeno M, Komatsu K, Kitazawa Y, Fujita N, et al. Recognition of floral homeotic MADS domain transcription factors by a phytoplasmal effector, phyllogen, induces phyllody. *Plant J.* 2014; 78: 541–554. doi: [10.1111/tbj.12495](https://doi.org/10.1111/tbj.12495) PMID: [24597566](https://pubmed.ncbi.nlm.nih.gov/24597566/)
4. Liu LY, Tseng HI, Lin CP, Lin YY, Huang YH, Huang CK, et al. High-throughput transcriptome analysis of the leafy flower transition of *Catharanthus roseus* induced by peanut witches'-broom phytoplasma infection. *Plant Cell Physiol.* 2014; 55: 942–957. doi: [10.1093/pcp/pcu029](https://doi.org/10.1093/pcp/pcu029) PMID: [24492256](https://pubmed.ncbi.nlm.nih.gov/24492256/)
5. Chung WC, Chen LL, Lo WS, Lin CP, Kuo CH. Comparative analysis of the peanut witches'-broom phytoplasma genome reveals horizontal transfer of potential mobile units and effectors. *PLOS ONE.* 2013; 8: e62770. doi: [10.1371/journal.pone.0062770](https://doi.org/10.1371/journal.pone.0062770) PMID: [23626855](https://pubmed.ncbi.nlm.nih.gov/23626855/)
6. Agüero J, Ruiz-Ruiz S, Del Carmen Vives M, Velázquez K, Navarro L, Peña L, et al. Development of viral vectors based on Citrus leaf blotch virus to express foreign proteins or analyze gene function in citrus plants. *Mol Plant Microbe Interact.* 2012; 25: 1326–1337. doi: [10.1094/MPMI-02-12-0048-R](https://doi.org/10.1094/MPMI-02-12-0048-R) PMID: [22670755](https://pubmed.ncbi.nlm.nih.gov/22670755/)
7. Collens JI, Mason HS, Curtis WR. Agrobacterium-mediated viral vector-amplified transient gene expression in *Nicotiana glutinosa* plant tissue culture. *Biotechnol Prog.* 2007; 23: 570–576. PMID: [17425328](https://pubmed.ncbi.nlm.nih.gov/17425328/)
8. Hanley K, Nguyen LV, Khan F, Pogue GP, Vojdani F, Panda S, et al. Development of a plant viral-vector-based gene expression assay for the screening of yeast cytochrome p450 monooxygenases. *Assay Drug Dev Technol.* 2003; 1: 147–160. PMID: [15090141](https://pubmed.ncbi.nlm.nih.gov/15090141/)
9. Harpaz-Saad S, Azoulay T, Arazi T, Ben-Yaakov E, Mett A, Shibolet Y, et al. Chlorophyllase is a rate-limiting enzyme in chlorophyll catabolism and is posttranslationally regulated. *Plant Cell.* 2007; 19: 1007–1022. PMID: [17369368](https://pubmed.ncbi.nlm.nih.gov/17369368/)
10. Hsu CH, Lin SS, Liu FL, Su WC, Yeh SD. Oral administration of a mite allergen expressed by zucchini yellow mosaic virus in cucurbit species downregulates allergen-induced airway inflammation and IgE synthesis. *J Allergy Clin Immunol.* 2004; 113: 1079–1085. PMID: [15208588](https://pubmed.ncbi.nlm.nih.gov/15208588/)
11. Lacomme C, Chapman S. Use of potato virus X (PVX)-based vectors for gene expression and virus-induced gene silencing (VIGS). *Curr Protoc Microbiol.* 2008; 16: Unit 16.11. doi: [10.1002/9780471729259.mc16i01s8](https://doi.org/10.1002/9780471729259.mc16i01s8) PMID: [18770535](https://pubmed.ncbi.nlm.nih.gov/18770535/)
12. Liu Y, Schiff M, Dinesh-Kumar SP. Virus-induced gene silencing in tomato. *Plant J.* 2002; 31: 777–786. PMID: [12220268](https://pubmed.ncbi.nlm.nih.gov/12220268/)
13. Anandalakshmi R, Pruss GJ, Ge X, Marathe R, Mallory AC, Smith TH, et al. A viral suppressor of gene silencing in plants. *Proc Natl Acad Sci USA.* 1998; 27: 13079–13084.
14. Kasschau KD, Carrington JC. A counterdefensive strategy of plant viruses: suppression of posttranscriptional gene silencing. *Cell.* 1998; 95: 461–470. PMID: [9827799](https://pubmed.ncbi.nlm.nih.gov/9827799/)
15. Ruiz-Ferrer V, Voinnet O. Viral suppression of RNA silencing: 2b wins the Golden Fleece by defeating Argonaute. *Bioessays.* 2007; 29: 319–323. PMID: [17373696](https://pubmed.ncbi.nlm.nih.gov/17373696/)
16. Haikonen T, Rajamäki ML, Valkonen JP. Improved silencing suppression and enhanced heterologous protein expression are achieved using an engineered viral helper component proteinase. *J Virol Methods.* 2013; 193: 687–692. doi: [10.1016/j.jviromet.2013.07.054](https://doi.org/10.1016/j.jviromet.2013.07.054) PMID: [23933077](https://pubmed.ncbi.nlm.nih.gov/23933077/)
17. Dhillon T, Chiera JM, Lindbo JA, Finer JJ. Quantitative evaluation of six different viral suppressors of silencing using image analysis of transient GFP expression. *Plant Cell Rep.* 2009; 28: 639–647. doi: [10.1007/s00299-009-0675-5](https://doi.org/10.1007/s00299-009-0675-5) PMID: [19198843](https://pubmed.ncbi.nlm.nih.gov/19198843/)
18. Minato N, Komatsu K, Okano Y, Maejima K, Ozeki J, Senshu H, et al. Efficient foreign gene expression in planta using a plantago asiatica mosaic virus-based vector achieved by the strong RNA-silencing suppressor activity of TGBp1. *Arch Virol.* 2014; 159: 885–896. doi: [10.1007/s00705-013-1860-y](https://doi.org/10.1007/s00705-013-1860-y) PMID: [24154949](https://pubmed.ncbi.nlm.nih.gov/24154949/)
19. Kung YJ, Lin PC, Yeh SD, Hong SF, Chua NH, Liu LY, et al. Genetic analyses of the FRNK motif function of Turnip mosaic virus uncover multiple and potentially interactive pathways of cross-protection. *Mol Plant Microbe Interact.* 2014; 27: 944–955. doi: [10.1094/MPMI-04-14-0116-R](https://doi.org/10.1094/MPMI-04-14-0116-R) PMID: [24804808](https://pubmed.ncbi.nlm.nih.gov/24804808/)
20. Wu HW, Lin SS, Chen KC, Yeh SD, Chua NH. Discriminating mutations of HC-Pro of zucchini yellow mosaic virus with differential effects on small RNA pathways involved in viral pathogenicity and symptom development. *Mol Plant Microbe Interact.* 2010; 23: 17–28. doi: [10.1094/MPMI-23-1-0017](https://doi.org/10.1094/MPMI-23-1-0017) PMID: [19958135](https://pubmed.ncbi.nlm.nih.gov/19958135/)
21. Gleba Y, Klimyuk V, Marillonnet S. Viral vectors for the expression of proteins in plants. *Curr Opin Biotechnol.* 2007; 18: 134–141. PMID: [17368018](https://pubmed.ncbi.nlm.nih.gov/17368018/)

22. Gleba Y, Marillonnet S, Klimyuk V. Engineering viral expression vectors for plants: the 'full virus' and the 'deconstructed virus' strategies. *Curr Opin Plant Biol.* 2004; 7: 182–188. PMID: [15003219](#)
23. Shamekova M, Mendoza MR, Hsieh YC, Lindbo J, Omarov RT, Scholthof HB. Tombusvirus-based vector systems to permit over-expression of genes or that serve as sensors of antiviral RNA silencing in plants. *Virology.* 2014; 452–453: 159–165.
24. Lin YY, Fang MM, Lin PC, Chiu MT, Liu LY, Lin CP, et al. Improving initial infectivity of the Turnip mosaic virus (TuMV) infectious clone by a mini binary vector via agro-infiltration. *Botanical Studies.* 2013; 54: 22.
25. Zhang X, Garreton V, Chua NH. The AIP2 E3 ligase acts as a novel negative regulator of ABA signaling by promoting ABI3 degradation. *Genes Dev.* 2005; 19: 1532–1543. PMID: [15998807](#)
26. Zhang X, Henriques R, Lin SS, Niu QW, Chua NH. Agrobacterium-mediated transformation of *Arabidopsis thaliana* using the floral dip method. *Nat Protoc.* 2006; 1: 641–646. PMID: [17406292](#)
27. Chiu MT, Lin CP, Lin PC, Lin SS. Enhancement of IgG purification by FPLC for a serological study on the Turnip mosaic virus P1 protein. *Plant Pathol Bull.* 2013; 22: 21–30.
28. Zhao Y, Dong W, Zhang N, Ai X, Wang M, Huang Z, et al. A wheat allene oxide cyclase gene enhances salinity tolerance via jasmonate signaling. *Plant Physiol.* 2014; 164: 1068–1076. doi: [10.1104/pp.113.227595](#) PMID: [24326670](#)
29. Carrió-Seguí A, García-Molina A, Sanz A, Peñarrubia L. Defective Copper Transport in the *copt5* Mutant Affects Cadmium Tolerance. *Plant Cell Physiol.* 2015; 56: 442–454. doi: [10.1093/pcp/pcu180](#) PMID: [25432970](#)
30. Huang CF, Yamaji N, Ma JF. Knockout of a bacterial-type ATP-binding cassette transporter gene, *AtSTAR1*, results in increased aluminum sensitivity in *Arabidopsis*. *Plant Physiol.* 2010; 153: 1669–1677. doi: [10.1104/pp.110.155028](#) PMID: [20498340](#)
31. Zwart MP, Willemsen A, Daròs JA, Elena SF. Experimental evolution of pseudogenization and gene loss in a plant RNA virus. *Mol Biol Evol.* 2014; 31: 121–134. doi: [10.1093/molbev/mst175](#) PMID: [24109604](#)
32. Mochizuki T, Ohki ST. Detection of plant virus in meristem by immunohistochemistry and in situ hybridization. *Methods Mol Biol.* 2015; 1236: 275–287. doi: [10.1007/978-1-4939-1743-3_20](#) PMID: [25287510](#)
33. Appiano A, Pennazio S. Electron microscopy of potato meristem tips infected with potato virus X. *J Gen Virol.* 1972; 14: 273–276. PMID: [4112038](#)
34. Kitajima EW, Costa AS. Association of pepper ringspot virus (Brazilian tobacco rattle virus) and host cell mitochondria. *J Gen Virol.* 1969; 4: 177–181.
35. Lin NS, Langenberg WG. Distribution of barley stripe mosaic-virus protein in infected wheat root and shoot tips. *J Gen Virol.* 1984; 65: 2217–2224.
36. Roberts DA, Christie RG, Archer MCJ. Infection of apical initials in tobacco shoot meristems by tobacco ringspot virus. *Virology.* 1970; 42: 217–220. PMID: [5460132](#)
37. Toussaint A, Dekegel D, Vanheule G. Distribution of *Odontoglossum* ringspot virus in apical meristems of infected *Cymbidium* cultivars. *Physiol Plant Pathol.* 1984; 25: 297–305.
38. Takeshita M, Koizumi E, Noguchi M, Sueda K, Shimura H, Ishikawa N, et al. Infection dynamics in viral spread and interference under the synergism between Cucumber mosaic virus and Turnip mosaic virus. *Mol Plant Microbe Interact.* 2012; 25: 18–27. doi: [10.1094/MPMI-06-11-0170](#) PMID: [21916556](#)